ACS APPLIED MATERIALS & INTERFACES

Research Article

www.acsami.org

The Influence of Surface Modification on Bacterial Adhesion to Titanium-Based Substrates

Martina Lorenzetti,*[,†,‡] Iztok Dogša,[§] Tjaša Stošicki,[§] David Stopar,[§] Mitjan Kalin,[∥] Spomenka Kobe,[†,‡] and Saša Novak[†,‡]

[†]Department of Nanostructured Materials, Jožef Stefan Institute, Jamova cesta 39, 1000 Ljubljana, Slovenia

[‡]Jožef Stefan International Postgraduate School, Jamova cesta 39, 1000 Ljubljana, Slovenia

[§]Department of Food Science and Technology, Biotechnical Faculty, University of Ljubljana, Večna pot 111, 1000 Ljubljana, Slovenia

[∥]Laboratory for Tribology and Interface Nanotechnology, Faculty of Mechanical Engineering, University of Ljubljana, Bogišičeva 8, 1000 Ljubljana, Slovenia

ABSTRACT: This study examines bacterial adhesion on titanium-substrates used for bone implants. Adhesion is the most critical phase of bacterial colonization on medical devices. The surface of titanium was modified by hydrothermal treatment (HT) to synthesize nanostructured TiO_2-anatase coatings, which were previously proven to improve corrosion resistance, affect the plasma protein adsorption, and enhance osteogenesis. The affinity of the anatase coatings toward bacterial attachment was studied by using a green fluorescent protein-expressing *Escherichia coli* (gfp-*E. coli*) strain in connection with surface photoactivation by UV irradiation. We also analyzed the effects of surface topography, roughness, charge, and wettability. The results suggested the dominant effects of the macroscopic surface topography, as well as microasperity at the surface roughness scale, which were produced during titanium machining, HT treatment, or both. Macroscopic grooves provided a preferential site for bacteria deposit within the valleys, while the microscopic roughness of the valleys determined the actual interaction surface between bacterium and substrate, resulting in an "interlocking" effect and undesired high bacterial adhesion on nontreated titanium. In the case of TiO_2-coated samples, the nanocrystals reduced the width between the microasperities and thus added nanoroughness features. These factors decreased the contact area between the bacterium and the coating, with consequent lower bacterial adhesion (up to 50% less) in comparison to the nontreated titanium. On the other hand, the pronounced hydrophilicity of one of the HT-coated discs after pre-irradiation seemed to enhance the attachment of bacteria, although the increase was not statistically significant ($p > 0.05$). This observation may be explained by the acquired similar degree of wetting between gfp-*E. coli* and the coating. No correlation was found between the bacterial adhesion and the ζ-values of the samples in PBS, so the effect of surface charge was considered negligible in this study.

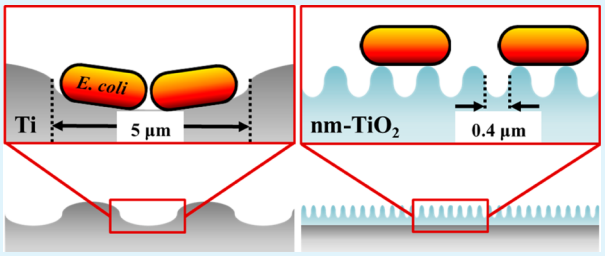

KEYWORDS: *titanium, titania, bone implants, anatase, coating, bacterial adhesion, photoactivation, roughness, topography*

INTRODUCTION

Over the past decade, the clinical demand for high-performance medical devices has contributed to a notable increase in research on biomaterials. In the field of hard tissue replacement, several significant steps have improved titanium-based implants in terms of mechanical properties (to resemble the healthy bone performances as much as possible), osseointegration (to overcome the bioinertness of the raw metals), corrosion resistance, and the rate of the release of metal ions (to avoid aseptic loosening of the implant).

Despite a generally good response by the body toward the Ti-based implants, bacteria may colonize on implant during the initial "race for the surface".[1] The relevant number of biomaterial-centered infections (BCI) and, more specifically, prosthetic implant infections (PIIs) represents a serious medical problem that significantly contributes to prosthetic implant failure and its aseptic loosening.[2,3] The primary cause of PIIs is presurgical contamination, which may result in infections within 3 months of implantation.[4] A 6 h post-implantation time is considered as the "decisive period" for implant surface colonization.[5] Chronic PIIs are usually due to the formation of a microbial biofilm. The biofilm is composed of bacteria that are attached to the surface and that become embedded in a self-made matrix of extracellular polymeric substances.[6] The nature of the biofilm structure confers resistance to antimicrobial agents and to a detachment by fluid flow. The resistant PIIs are usually resolved only by surgical removal of the implant. Bacterial adhesion to implant surfaces is a crucial first step in biofilm formation, which precedes clinical infection. The most common approaches for

Received: October 16, 2014
Accepted: December 26, 2014
Published: December 26, 2014

DOI: 10.1021/am507148n
ACS Appl. Mater. Interfaces 2015, 7, 1644−1651

avoiding infections of the inserted material are based on application of antimicrobial agents (either antistatic or bactericidal), applications of cytokines/chemokines, or incorporation of silver.[7,8] The acquired resistance to antibiotics and the pharmacokinetics decrease over time (high release rate) are the main drawbacks of this strategy. The most critical phase during the bacterial colonization of an implant is the bacterial adhesion on its surface; therefore, the antiadherent approach used in this work may eventually result in a higher success rate of transplantation.

The reversible/irreversible adhesion stage is largely influenced by the topographical features on the surface;[9,10] accordingly, several micro- or nanostructured titanium surfaces have been proposed.[11−13] However, much less is known about the ability and mechanisms of surface sensing by bacteria than eukaryotic cells.[14]

Indeed, surface chemistry and functional groups on the surface also influence bacterial adhesion. Several antiadherent coatings on titanium have been created by surface modification with polymers, copolymers, or proteins (e.g., silk sericin[15]). It has also been shown that bacterial adhesion is influenced by the crystalline phase of the titanium oxide present on the surface.

The application of TiO_2 anatase coatings on the Ti-implant surface is one of the best ways to enhance the interactions between the material and the biological environment at the interface. Del Curto et al.[16] reported that an anatase layer significantly reduced bacterial attachment with respect to the amorphous titania layer, without adverse effects on the cell metabolic activity. The same assumption was used by Puckett et al.[17] to support the improved bacterial adhesion on amorphous nanotubular and nanotextured structures on titanium, compared to conventional and nanorough surfaces, which contain rutile and anatase, respectively. Among the several methods proposed for the surface modification, hydrothermal treatment has been shown to be a promising technique to directly grow phase-pure, nanocrystalline coatings firmly attached to the substrate.[18] Moreover, the versatility, ease of use, cost-effectiveness and potential for scale-up make the HT synthesis very appealing in the field of orthopedics and orthodontics. Recently, we have reported about novel hydrothermally synthesized coatings, which have increased corrosion resistance and surface stability compared to the nontreated titanium (Ti NT) surface.[19] Moreover, the photocatalytic nature of the nanocrystalline anatase coatings improved the bioperformances of the titanium substrate upon photoinduction by UV light. The photoactivated surfaces reduced the adsorption of inflammation-promoter plasma proteins[20] and increased the bioactivity and osteogenesis due to the positive interaction of human mesenchymal stem cells with the HT coatings.[21]

An alternative approach introduces functionalities onto the Ti-based implant surfaces, which can reduce the biocontamination level, improve the ability to self-clean, or both. The photoinduced phenomena occurring on TiO_2 surfaces upon UV irradiation are currently under study by several research groups who have reported the potential bactericidal effect of titania coatings under UV light (photokilling).[22−24] As demonstrated in our previous work,[25] hydrothermally grown anatase coatings exhibited photocatalytic activity and photoinduced superhydrophilicity.[26] If the photocatalytic activity is related to the photokilling effect, the superhydrophilicity may play an important role in the bacterial adhesion process, which is significantly affected by surface wettability.[27,28] Gallardo-Moreno et al.[29] observed that the UV irradiation of Ti6Al4V facilitated the removal of most of the adhered bacteria by shear forces. Moreover, it is commonly accepted that surface topography and surface roughness have a strong influence on the bacterial adhesion.[9]

The aim of this study was to verify the extent of *Escherichia coli* adhesion on hydrothermally treated titanium, with or without preirradiation, in comparison to the nontreated titanium substrate. The adhesion results were correlated with topographical, electrostatic and hydrophobic/hydrophilic properties of bacteria and material surfaces.

EXPERIMENTAL SECTION

Hydrothermal Synthesis. Hydrothermal treatments (HT) were performed on commercially pure titanium (cp Ti grade 2, ASTM F67, Pro-Titanium, China), mechanically machined as discs with a diameter of 15 mm and thickness of 2 mm. For the HT, two different aqueous suspensions containing titanium(IV) isopropoxide $(Ti(iOPr)_4$, Acros Organics) were prepared: the first suspension (sample TiA) had no other additives and a pH of 5; the pH of the second suspension (sample TiB) was adjusted to 10 with tetramethylammonium hydroxide (TMAH, Sigma-Aldrich Chemie GmbH, Germany). Both suspensions were then transferred in two Teflon vessels containing the Ti-discs and placed in steel autoclaves. The autoclave containing the TiA suspension was heated at 200 °C for 24 h, while the autoclave with the TiB suspension was heated at 200 °C for 48 h. Discs of Ti NT were used as machined for comparison.

Characterization. The TiO_2-anatase crystal morphology was imaged by field-emission scanning electron microscopy (FE-SEM, Zeiss SUPRA 35VP, Carl Zeiss SMT, Germany and JEOL JSM 7600F, Japan). The crystal size was estimated from the SEM micrographs processed by ImageJ 1.48v software; the estimation was done by considering the distribution of the main axis, after fitting the crystals with ellipses.

The surface macroscopic topography was analyzed using white light interferometry (Contour GT Ko, Bruker, Billerica, MA) at 240 × 180 μm scans. The surface within the valleys was additionally measured in both the parallel and perpendicular directions in macroscopic grooves to analyze the local asperity features and determine the roughness. Average roughness (R_a) values and standard deviation from both directions are reported in the Results section.

Zeta potential (ζ) analyses were carried out by an electrokinetic analyzer (SurPASS, Anton Paar GmbH, Austria). The pH dependence of ζ-potential (titration curves) and the isoelectric point (IEP) were obtained in 0.001 mol/L phosphate buffer saline solution (PBS, tablets, Sigma-Aldrich). For the purpose of this work, only the ζ-values at physiological pH (pH = 7.4) were considered.

The sessile drop contact angles (CA) on the surfaces were measured, as an indication of the wettability of the substrates. Droplets of deionized water (volume ≈ 4 μL) were deposited at different positions on the surfaces, and their profiles were captured and analyzed by a Theta Lite T101 optical tensiometer (Attension, Biolin Scientific, Finland). The results are presented as the mean contact angles of at least five droplet measurements per sample, with their standard deviation.

To verify the photoactivation effect, we performed the CA measurements before and after 5 h of irradiation of the samples under UV light. The preirradiation of the substrates was achieved by using a UVB portable lamp (Dual 302 nm Wavelength Light Tubes Lamp, 8 W, 2000 $\mu W/cm^2$, Cole-Parmer) at ≈10 cm working distance.

Carpets of bacteria were obtained by filtering 1 or 2 mL of bacterial inoculum (see Bacterial Adhesion Testing) on 0.2 μm GTBP membrane filters (Millipore) and used for the wetting measurements. The contact angle of the obtained lawns was measured every 30 min for the first 5 h and after 20 h.

Bacterial Adhesion Testing. Green fluorescent protein-expressing *Escherichia coli* strain MG 1655, DE3 (gfp-*E. coli*) was used for the purpose of this study. *E. coli* was cultured on Luria broth (LB, Sigma-Aldrich) agar plates, supplemented with 50 μg/mL kanamycin sulfate

DOI: 10.1021/am507148n
ACS Appl. Mater. Interfaces 2015, 7, 1644−1651

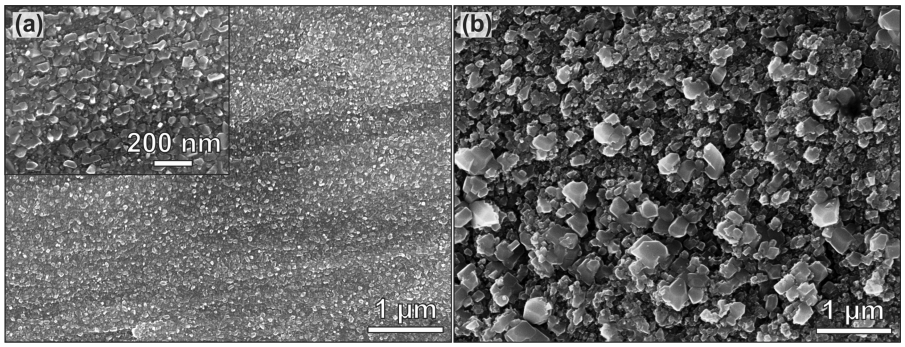

Figure 1. SEM micrographs of (a) TiA and (b) TiB.

Table 1. Surface Properties of Titanium Non-Treated (Ti NT), Hydrothermally Treated Coatings (TiA and TiB) and gfp-*E. coli* (MG 1655, DE3)

surface property		gfp-*E. coli*	Ti NT	TiA	TiB
estimated crystal size (nm)				20−70	50−100
					200−400
micro-waviness peak-to-valley height (μm)			0.7 ± 0.1	1.0 ± 0.2	1.5 ± 0.2
micro-roughness, R_a (μm)			0.31 ± 0.09	0.45 ± 0.08	0.80 ± 0.14
microwaviness peak-to-peak distance (μm)			5.0 ± 0.4	3.0 ± 0.3	0.4 ± 0.1
WCA	no irr.	14° ± 3°	63° ± 4°[a]	56° ± 2°[a]	30° ± 6°[a]
	UV preirr.		67° ± 5°[a]	34° ± 6°[a]	19° ± 0°[a]
ζ (mV) at pH = 7.4		−50[b]	−81[a]	−54[a]	−65[a]

[a]Data from Lorenzetti et al.[20] [b]*E. coli* (D21) in PBS (0.001 mol/L), data from Li et al.[32]

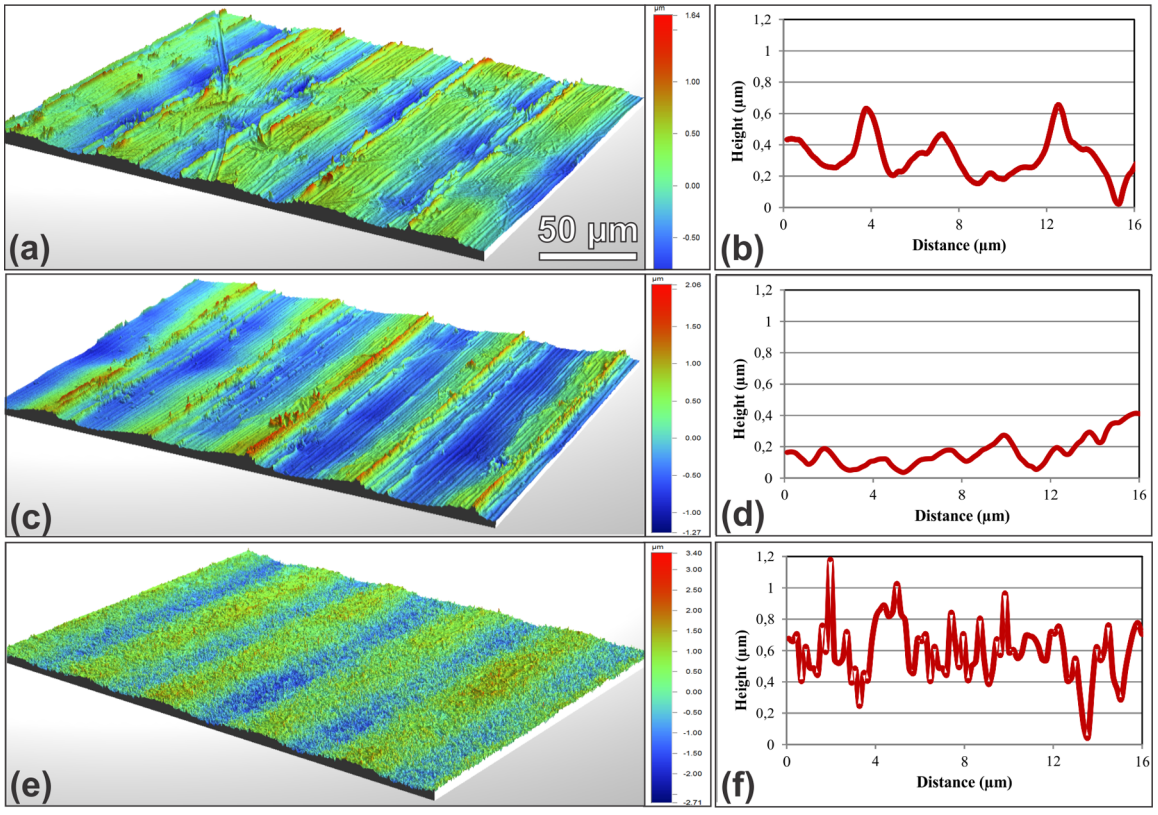

Figure 2. 3D and 2D optical interferometry images revealing (left) macro-waviness and (right) microwaviness features of (a and b) Ti NT, (c and d) TiA, and (e and f) TiB.

from *Streptomyces kanamyceticus* (KM, Sigma-Aldrich). The overnight cultures were prepared in 25 mL of LB medium with 50 μg/mL KM and incubated at 37 °C with shaking at 200 rpm. The next day, an aliquot (500 μL) of overnight culture was used to inoculate 25 mL of

DOI: 10.1021/am507148n
ACS Appl. Mater. Interfaces 2015, 7, 1644−1651

fresh LB medium enriched with 50 μg/mL of KM. The culture was grown at 37 °C at 200 rpm shaking until the optical density (OD_{650}) of the culture reached 0.7 (~2.5 h). At OD_{650} = 0.7, isopropyl β-D-1-thiogalactopyranoside (IPTG, Thermoscientific; 5 μg/mL) was added, and the incubation was kept for an additional 1 h at 37 °C at 200 rpm shaking. The bacterial culture was then transferred to 1.5 mL microcentrifuge tubes, centrifuged for 5 min at 7000 rpm, and resuspended in 1:500 LB/PBS solution. A sample (2 μL) of the bacteria solution was used to count the bacteria concentration by light microscopy using the phase-contrast technique (Zeiss Axio Observer Z1 equipped with an AxioCam MRm Rev.3 camera). After bacteria counting, the culture was diluted in 1:500 LB/PBS to the concentration of approximately 2×10^8 bacteria/mL. The resuspended bacteria were prestained with 500 times diluted propidium iodide (B dye, The Live/Dead BacLight bacterial viability kit, Molecular probes) in 1:1 ratio.

The adhesion test was performed in a closed system (centrifuge tube placed upside-down), using either nonirradiated or preirradiated with UVB light (Dual 302 nm Wavelength Light Tubes Lamp, 8 W, 2000 $\mu W/cm^2$, Cole-Parmer) for 5 h.

Samples (10 μL) of gfp-*E. coli*, prestained with propidium iodide, were added on each disc previously placed in the sterile cap of an upside-down 50 mL centrifuge tube and covered by a cover glass. In order to protect bacteria from drying, 500 μL of deionized water was placed in the cap. The sealed centrifuge tube was then incubated at 37 °C in the dark for 1 h. After incubation, the discs were washed by vortex stirring (IKA MS3 digital) in 5 mL of PBS for 1 min at 1000 rpm to remove the nonadhered or weakly adhered bacteria.

Bacteria Imaging and Quantification on the Discs. Adhesion of bacteria on different types of material was observed using an inverted fluorescent microscope Zeiss Axio Observer Z1 equipped with an AxioCam MRm Rev.3 camera. The samples were observed under 10× magnification. For the detection of green fluorescent protein and propidium iodide, the used filters were 38 HE and 43 HE (Zeiss), respectively. The Mosaix function of Axiovision software (Zeiss) allowed capture of a surface area of 11 mm^2, which covered 1/10 of the disc area. The captured images were analyzed with ImageJ (Version 1.43u) software. Since some gfp-*E. coli* bacteria were fluorescent under both 38 HE and 43 HE filters, a parallel experiment with the live/dead staining (Live/Dead BacLight bacterial viability kit, Molecular Probes) was performed on a fresh culture; the green and red intensities were used to determine the threshold between live and dead bacteria, respectively.

All samples were tested in at least four independent experiments. Within each experiment, each sample was replicated at least twice. All the bacterial adhesion data are presented as the average values of bacteria adhered to the surface, relative to the total amount of added bacterial cells. The experimental error is given by standard errors. The Student's *t*-test assuming unequal variances was applied to test the significance of the results. The significance of the results is reported at $p < 0.05$.

RESULTS

Surface Physicochemical Properties. The two hydrothermal (HT) synthesis routes led to the growth of two different nanosized TiO_2-anatase coatings (Figure 1). As reported in our previous work[25] and in accordance with literature data,[30,31] the use of TMAH as a pH modifier highly influenced the crystal growth and morphology. The variation in crystal size and morphology generated different surface properties with respect to the bare titanium (Table 1).

As shown in Figure 2, the samples presented topographical features at two levels. The mechanical machining provided regular grooves of about 30 μm width and about 0.5−1 μm high on all the titanium substrates (Figure 2a,c,e). The topography changed when the HT was applied; the average peak-to-valley value between the macroscopic grooves increased from 0.7 μm for Ti NT to 1 μm for the TiA sample and 1.5 μm for the TiB sample (Table 1).

Within a single groove, however, a second level of surface microtopography features, that is, the actual roughness, as well as microwaviness, can be distinguished (Figure 2b,d,f) and quantified (Table 1). The R_a roughness values follow the same trend of the microscopic topographic average peak-to-valley waviness; they are the least for Ti NT (0.31 μm), intermediate for TiA (0.45 μm), and the highest for TiB (0.80 μm). Moreover, characteristic distances between the asperities of microwaviness (Figure 2b,d,f) were noticed and measured in the direction parallel to macro-waviness (macro-grooves). The distance between microwave peaks revealed that the Ti NT surface presented μm-sized asperities of 5 μm width. However, in case of HT-coatings, the presence of nanocrystals diminished the peak-to-peak distance between the asperities, down to 3 μm for TiA and even as small as 0.4 μm for TiB (Table 1). The different sizes of the nanocrystals (Table 1) explain the changed values in roughness for TiA and TiB. The topography did not change upon UV irradiation (data not shown).

All the Ti-based surfaces were hydrophilic (CA < 90°) and negatively charged within the range between −54 mV and −81 mV at physiological pH in PBS solution (Table 1). The HT reduced the magnitude of the net surface charge and increased the wettability of the substrate, lowering the ζ and CA values for both coatings but to a different extent. The UV preirradiation enhanced even more the hydrophilic character (−40% CA compared to nonirradiated HT-coatings) by the occurrence of the photoinduced wettability phenomenon, as shown in our previous work.[25] This effect was not achieved on preirradiated Ti NT.

Bacterial Adhesion. To evaluate *E. coli* adhesion to different surfaces (Figure 3), we incubated bacteria in the midexponential growth phase in contact with the surfaces for 1 h; after incubation, the titanium discs were vortex-stirred in 5 mL of PBS for 1 min at 1000 rpm to remove the nonadhered or weakly adhered bacteria. The distribution of strongly adhered bacteria was nonhomogeneous over the entire surface. We then

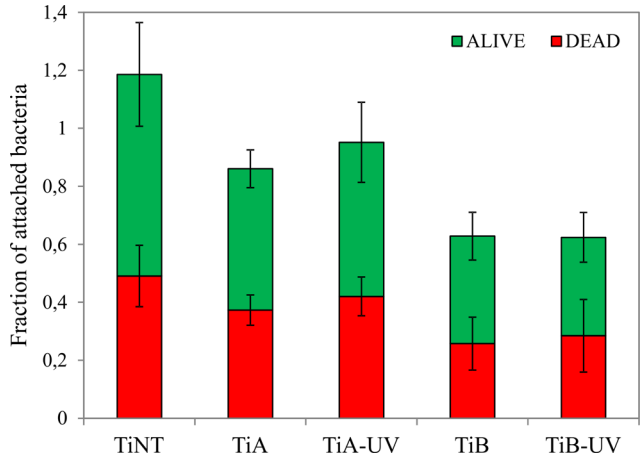

Figure 3. Fraction of gfp-*E. coli* bacteria attached to different surfaces. The magnitude of the bars represents the total amount of adhered bacteria; (green) fraction of live bacteria and (red) fraction of dead bacteria. TiNT, titanium substrate, no additional treatment; TiA, hydrothermally treated titanium at 200 °C for 24 h, suspension pH 5.0; TiB, hydrothermally treated titanium at 200 °C for 48 h, suspension pH 10.0; TiA-UV and TiB-UV, hydrothermally treated titanium preirradiated for 5 h under UVB light.

DOI: 10.1021/am507148n
ACS Appl. Mater. Interfaces 2015, 7, 1644−1651

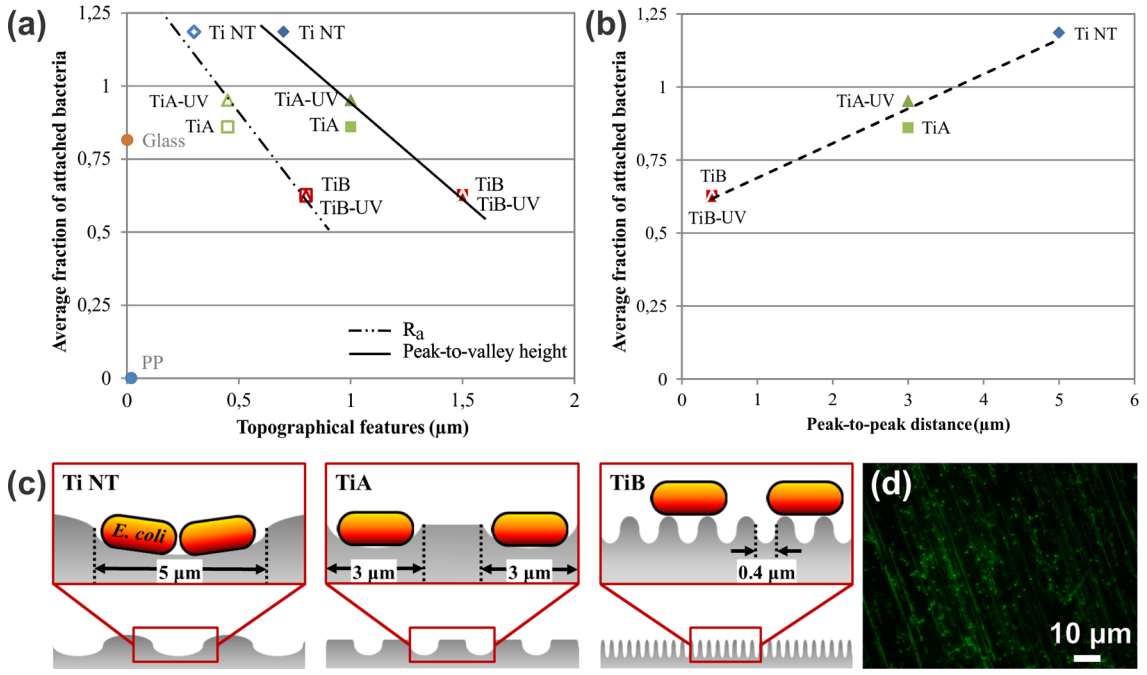

Figure 4. Average fraction of adhered bacteria on Ti NT, TiA, TiA-UV, TiB, and TiB-UV samples versus (a) peak-to-valley height (filled symbols) and R_a roughness (open symbols) within the machined grooves in comparison with glass and polypropylene (PP) surfaces and (b) peak-to-peak distance. (c) Height versus distance profiles for Ti NT, TiA, and TiB samples. (d) Gfp-*E. coli* stained with Live/Dead kit on Ti NT.

visually inspected approximately $^1/_{10}$ of the disc area to obtain appropriate statistical analyses. The total amount of adhered bacteria was dependent on the properties of the surface. In the case of the nontreated titanium surface, all added bacteria strongly adhered to the surface. In a comparison of live to dead cells, the fraction of attached bacteria in nontreated titanium exceeded a value of 1.0 and can be attributed to residual growth after the cells had been counted, diluted, and attached to the surface. This residual growth increased the total count of bacteria by up to 20%. After attachment to the surface, no growth of bacteria was observed. Hydrothermal treatment of titanium surfaces decreased the number of bacteria attached to the surface, but only in the case of sample TiB, maintained at pH 10, was the decrease statistically significant (47% less in comparison to Ti NT). UV irradiation increased the number of attached cells in case of TiA-UV, but the increase was not significant. There was no further effect of UV treatment in the case of TiB-UV sample. Upon adhesion to the surface, a large fraction of bacteria died. The fraction of dead bacteria varied between 40 and 45% on different surfaces. The hydrothermal treatment or UV pretreatment did not change the fraction of dead cells.

DISCUSSION

Although the traditional approach of using chemical antimicrobial agents to control biofilm formation is widely used, problems with antibiotic resistance and low efficiency of antimicrobials in biofilms have led to the need for new engineered materials.

On the basis of the state-of-the-art research reviewed in the Introduction, we hypothesized that the hydrothermally treated nanocrystalline anatase coatings on titanium would favor the inhibition of bacterial adhesion due to the peculiar topography and good wettability of these coatings, especially after UV photoactivation. Therefore, in this study the correlation between surface topography, electrostatic, and hydrophilic/hydrophobic interactions in the bacterium−substrate system was studied to gain insights into the *E. coli* adhesion process.

As shown in Figures 1 and 2, the topography of the titanium machined surfaces developed in multiple levels of complexity from a macro- toward a micro- and nanolevel and changed in accordance to the HT treatment. Both the peak-to-valley height and the profile mean roughness (R_a) within the groove valleys increased within the series Ti NT < TiA < TiB, following the order of TiO_2 nanocrystal size (Table 1). Interestingly, the relative number of bacteria was inversely proportional to these values (Figure 4a). This relationship was valid, however, only within the group of Ti-based substrates, because behavior independent of the surface roughness was observed for other materials (glass and polypropylene foil, PP).

The parameter of the microwaviness peak-to-peak distance within the machined macro-grooves was also crucial to understanding the bacterial behavior on titanium. Although the size of crystal grains was 10 times smaller in TiA compared to TiB, the microwaviness peak-to-peak distance was approximately 10 times larger in TiA and influenced the contact area between the material and bacterial surface. The ∼30 μm microgrooves width was due to machining, which was the same for all surfaces. However, a detailed profile analysis revealed that within such widths, another type of microtopography existed, with significantly different values depending on the materials studied. The trend of the values proportionally followed the bacterial adhesion sequence (Figure 4b). For the Ti NT, the distance between the peak-to-peak microwaves was about 5 μm in width and this distance grew smaller with hydrothermal treatment due to the presence of nanocrystals. The bigger the crystals appeared, the smaller was the peak-to-peak microwaviness distance. Accordingly, the TiA coating offered 3 μm gaps, while TiB displayed only 0.4 μm gaps, which is significantly less than bacteria size (Table 1).

DOI: 10.1021/am507148n
ACS Appl. Mater. Interfaces 2015, 7, 1644−1651

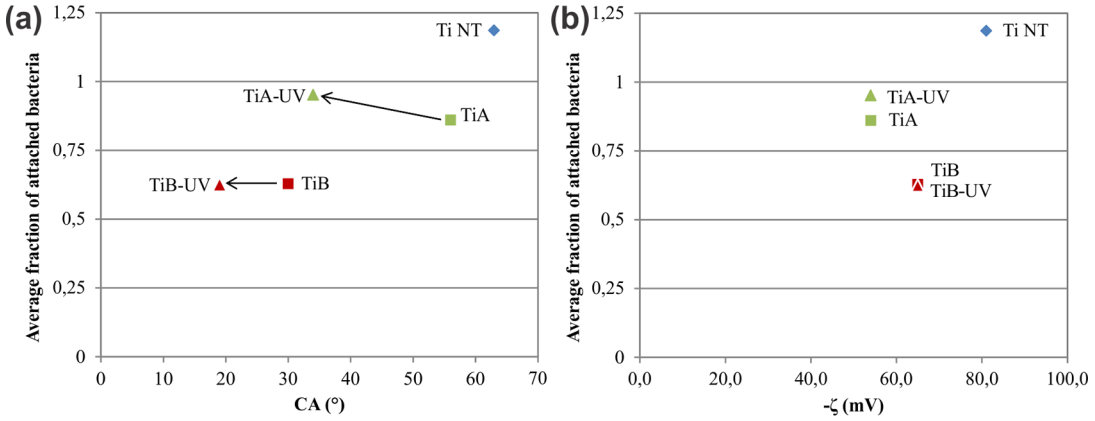

Figure 5. Average fraction of adhered bacteria on Ti NT, TiA, TiA-UV, TiB and TiB-UV samples versus (a) water contact angle values (CA) and (b) absolute zeta potential values (ζ).

Considering the peak-to-peak parameter, the trend within the Ti-based samples was directly proportional to the bacterial adhesion (Figure 4b). This outcome becomes clear if the peak-to-peak distances are compared to the bacteria dimensions. Gfp-*E. coli* can be represented as a rod of approximately 2 × 1 μm. Accordingly, up to 2 bacteria could theoretically lie within the 5 μm width asperities of Ti NT; following the same criterion, only 1 bacterium could lie within the 3 μm width asperities of TiA. In the case of TiB, none of the bacteria could penetrate within the gaps because the gap width was too small (Figure 4c). Therefore, such subgroove dimensions allowed bacterial adhesion on all the surfaces, due to a sufficient groove depth to "hide" and protect bacteria from direct exposure to the external forces. However, only Ti NT and TiA had the proper μm-topography to offer the maximum contact area between *E. coli* and the surface, most probably causing the "interlocking" effect to occur. On the other hand, the 0.4 μm gaps offered only contact-points for the bacterial adhesion on TiB surface, resulting in the least bacterial adhesion (about 50% less in comparison to Ti NT) due to the lower real contact area, which is proportional to adhesive force (Figure 4c). The preferential adhesion within the microasperities is illustrated in Figure 4d.

In addition to the surface topography and roughness, the presence of hydrophobic surfaces increases the number of attached bacteria as compared to hydrophilic surfaces.[12,27,33] As shown in Table 1, both the hydrothermal and UV treatment increased the hydrophilic character of the titanium surface. According to general thermodynamic theory,[27] the increased hydrophilicity of hydrothermally and UV-treated samples should reduce the number of adhered bacteria compared to Ti NT, and our observations confirmed this prediction. However, the effect of UV photoinduced wettability was not statistically significant (Figure 5a), when compared to non-UV-treated samples. This result is at odds with the study by Gallardo-Moreno et al.,[29] in which UVC-irradiated Ti6Al4V alloy reduced bacterial adhesion. Two main differences have to be pointed out: first, polished surfaces were used by Gallardo-Moreno et al.[29] instead of machined ones. Second, when comparing TiA with TiA-UV and TiB with TiB-UV, the surface wettability of gfp-*E. coli* (CA = 14°) must be taken into account. The hydrophilic interactions among surfaces with similar hydrophilic character may explain the slight tendency (although not significant) of improved bacterial adhesion on TiA-UV (CA = 34°) rather than on TiA nonirradiated (CA = 56°). We believe the use of different bacterial species accounts for the difference between these two studies. Both *Staphylococcus aureus* and the two species of *Staphylococcus epidermidis* used by Gallardo-Moreno[29] are much more hydrophobic (CA = 72, 74, and 58°, respectively) than the *E. coli* used in our study (CA = 14°), resulting in a dissimilar interaction with the hydrophilic alloy surface. These results suggest that the role of topography can overcome the effect of surface hydrophilicity.

The microbial adhesion phase also depends on the electrostatic interactions between the surface of the material and the surface of the bacterium coming in contact, factors which are not included in the thermodynamic theory. For this reason, the surface charge of both bacteria and materials should not be neglected in predicting bacterial adhesion on biomaterial substrates.[32] According to the DLVO theory,[34] the particle adhesion is affected by long-range interactions which include Lifshitz-van der Waals interactions and interactions resulted from the overlapping electric double layers. In the extended XDLVO theory,[35] additional short-range Lewis acid−base or hydration interactions have also been taken into account. The bacterial cell surface structure is complex and there are many known deviations from the DLVO and XDLVO theories in the bacterial adhesion studies. The theory works well only if the free energy of the binding process is negative, that is, if we have an electrostatic attraction. In the case of two negatively charged surfaces, as with negatively charged titanium surfaces and negatively charged bacterial surfaces, the simple DLVO theory does not work well. If one goes beyond the zeta-potential, the electrostatic potential decreases to zero. Nevertheless, the adhesive long-range van der Waals forces may extend up to 50 nm, which is at least 1 order of magnitude less than the microroughness scale (important in the initial phases of bacterial adhesion). It is only when bacteria approach the surface that the effect of electrostatic interactions become progressively more important. All the analyzed samples appeared negatively charged in PBS, with ζ in the range of −54 to −81 mV; a general electrostatic repulsion toward the negatively charged gfp-*E. coli* (−50 mV) might be expected to occur. Also, stronger repulsion of bacteria could be expected for the Ti NT sample, characterized by the highest negative charge (−81 mV). However, no relationship between the number of bacteria and the ζ could be found (Figure 5b), which is probably the consequence of the prevailing effect of roughness. In this regard, materials with significantly different surface charges, including positive polarity, will be considered in further

DOI: 10.1021/am507148n
ACS Appl. Mater. Interfaces 2015, 7, 1644−1651

study to verify this correlation. In addition, although the results of this study suggest that the hydrothermally modified Ti-based surfaces may reduce bacterial adhesion, in a more complex environment the adhesion of bacteria may be significantly modified by proteins or other polymers that condition the substrate in the "race for the surface".

CONCLUSIONS

This study demonstrated that the hydrothermally synthesized TiO_2-anatase coatings, which were previously proved as advantageous in terms of corrosion resistance, inflammatory potential and osteogenesis, also significantly reduced the *E. coli* adhesion on the surface (about 50% less for TiB versus Ti NT), which is due to a distinctive combination of surface properties and parameters, especially topography and roughness. This capability is retained also after UV preirradiation of the coatings.

Because bacterial adhesion is a multifactored process, the correlation between the surface characteristics and the bacterial affinity to them was studied from the point of view of surface topography (roughness), wettability and surface charge. The results demonstrated that the effect of surface topography on bacterial attachment was predominant, with only minor contributions from the wetting and surface charge. When the peak-to-peak distances were approximately equal to (TiA) or larger than (Ti NT) the bacteria size, the bacterial attachment was favored. In contrast, the structures with fine asperities (TiB) reduced the contact area and, hence, the number of successfully attached bacteria despite its high hydrophilicity. This trend was not significantly affected by UV-induced hydrophilicity of the HT surfaces.

AUTHOR INFORMATION

Corresponding Author

*E-mail: martina.lorenzetti@ijs.si. Phone: +386 1 4773 931. Fax: +386 1 4773 221.

Author Contributions

The manuscript was written through contributions of all authors. All authors have given approval to the final version of the manuscript.

Notes

The authors declare no competing financial interest.

ACKNOWLEDGMENTS

Funding by the European Commission within the framework of the FP7-ITN network BioTiNet (FP7-PEOPLE-2010-ITN-264635) is acknowledged. The authors wish to thank Dr. Aljaž Ivekovič and Mr. Matej Kocen for the assistance during the zeta potential measurements and Miss Špela Koželj for the help with the bacteria cultures. The authors acknowledge Dr. Rok Simič for the topography measurements and Miss Mateja Košir for the crystal size measurements.

ABBREVIATIONS

BCI, biomaterial centered infections
DLVO, Derjaguin−Landau−Verwey−Overbeek theory
gfp-*E. coli*, green fluorescent protein-expressing *Escherichia coli*
HT, hydrothermal treatment
IPTG, isopropyl β-D-1-thiogalactopyranoside
KM, kanamycin sulfate
LB, Luria broth
NT, nontreated
PBS, phosphate buffer saline solution
PEI, polyethylenimine
PII, prosthetic implant infections
PP, polypropylene
R_a, profile mean roughness
Ti, titanium
TiA, hydrothermally treated titanium at 200 °C for 24 h, suspension pH 5.0
TiA-UV, sample TiA preirradiated for 5 h under UVB light
TiB, hydrothermally treated titanium at 200 °C for 48 h, suspension pH 10.0
TiB-UV, sample TiB preirradiated for 5 h under UVB light
UV, ultraviolet
WCA, water contact angle
XDLVO, extended Derjaguin−Landau−Verwey−Overbeek theory
ζ, zeta potential

REFERENCES

(1) Gristina, A. G.; Naylor, P.; Myrvik, Q. Infections from Biomaterials and Implants: A Race for the Surface. *Med. Prog. Technol.* **1988**, *14*, 205−224.
(2) Brady, R.; Calhoun, J.; Leid, J.; Shirtliff, M. *Infections of Orthopaedic Implants and Devices*. Springer: Berlin, 2008; pp 1−41.
(3) Gottenbos, B.; Busscher, H. J.; Van Der Mei, H. C.; Nieuwenhuis, P. Pathogenesis and Prevention of Biomaterial Centered Infections. *J. Mater. Sci.: Mater. Med.* **2002**, *13*, 717−722.
(4) Kaltsas, D. S. Infection after Total Hip Arthroplasty. *Ann. R. Coll. Surg. Engl.* **2004**, *86*, 267−271.
(5) Rodrigues, L. R. Inhibition of Bacterial Adhesion on Medical Devices. *Adv. Exp. Med. Biol.* **2011**, *715*, 351−367.
(6) Donlan, R. M.; Costerton, J. W. Biofilms: Survival Mechanisms of Clinically Relevant Microorganisms. *Clin. Microbiol. Rev.* **2002**, *15*, 167−193.
(7) Goodman, S. B.; Yao, Z.; Keeney, M.; Yang, F. The Future of Biologic Coatings for Orthopaedic Implants. *Biomaterials* **2013**, *34*, 3174−3183.
(8) Zhao, L.; Chu, P. K.; Zhang, Y.; Wu, Z. Antibacterial Coatings on Titanium Implants. *J. Biomed. Mater. Res., Part B* **2009**, *91B*, 470−480.
(9) Crawford, R. J.; Webb, H. K.; Truong, V. K.; Hasan, J.; Ivanova, E. P. Surface Topographical Factors Influencing Bacterial Attachment. *Adv. Colloid Interface Sci.* **2012**, *179−182*, 142−149.
(10) Ivanova, E. P.; Truong, V. K.; Wang, J. Y.; Berndt, C. C.; Jones, R. T.; Yusuf, I. I.; Peake, I.; Schmidt, H. W.; Fluke, C.; Barnes, D.; Crawford, R. J. Impact of Nanoscale Roughness of Titanium Thin Film Surfaces on Bacterial Retention. *Langmuir* **2009**, *26*, 1973−1982.
(11) Truong, V. K.; Lapovok, R.; Estrin, Y. S.; Rundell, S.; Wang, J. Y.; Fluke, C. J.; Crawford, R. J.; Ivanova, E. P. The Influence of Nano-Scale Surface Roughness on Bacterial Adhesion to Ultrafine-Grained Titanium. *Biomaterials* **2010**, *31*, 3674−3683.
(12) Braem, A.; Van Mellaert, L.; Mattheys, T.; Hofmans, D.; De Waelheyns, E.; Geris, L.; Anné, J.; Schrooten, J.; Vleugels, J. Staphylococcal Biofilm Growth on Smooth and Porous Titanium Coatings for Biomedical Applications. *J. Biomed. Mater. Res., Part A* **2014**, *102*, 215−224.
(13) Wu, Y.; Zitelli, J. P.; TenHuisen, K. S.; Yu, X.; Libera, M. R. Differential Response of Staphylococci and Osteoblasts to Varying Titanium Surface Roughness. *Biomaterials* **2011**, *32*, 951−960.
(14) Anselme, K.; Davidson, P.; Popa, A. M.; Giazzon, M.; Liley, M.; Ploux, L. The Interaction of Cells and Bacteria with Surfaces Structured at the Nanometre Scale. *Acta Biomater.* **2010**, *6*, 3824−3846.
(15) Zhang, F.; Zhang, Z.; Zhu, X.; Kang, E. T.; Neoh, K. G. Silk-Functionalized Titanium Surfaces for Enhancing Osteoblast Functions and Reducing Bacterial Adhesion. *Biomaterials* **2008**, *29*, 4751−4759.

DOI: 10.1021/am507148n
ACS Appl. Mater. Interfaces 2015, 7, 1644−1651

(16) Del Curto, B.; Brunella, M. F.; Giordano, C.; Pedeferri, M. P.; Valtulina, V.; Visai, L.; Cigada, A. Decreased Bacterial Adhesion to Surface-Treated Titanium. *Int. J. Artif. Organs* **2005**, *28*, 718−730.
(17) Puckett, S. D.; Taylor, E.; Raimondo, T.; Webster, T. J. The Relationship between the Nanostructure of Titanium Surfaces and Bacterial Attachment. *Biomaterials* **2010**, *31*, 706−713.
(18) Drnovsek, N.; Daneu, N.; Recnik, A.; Mazaj, M.; Kovac, J.; Novak, S. Hydrothermal Synthesis of a Nanocrystalline Anatase Layer on Ti6Al4V Implants. *Surf. Coat. Technol.* **2009**, *203*, 1462−1468.
(19) Lorenzetti, M.; Pellicer, E.; Sort, J.; Baró, M.; Kovač, J.; Novak, S.; Kobe, S. Improvement to the Corrosion Resistance of Ti-Based Implants Using Hydrothermally Synthesized Nanostructured Anatase Coatings. *Materials* **2014**, *7*, 180−194.
(20) Lorenzetti, M.; Bernardini, G.; Luxbacher, T.; Santucci, A.; Kobe, S.; Novak, S. Surface Properties of Nanocrystalline TiO_2 Coatings in Relation to the in Vitro Plasma Protein Adsorption. *Biomed. Mater.* **2014**, submitted for publication.
(21) Lorenzetti, M.; Dakischew, O.; Trinkaus, K.; Lips, K. S.; Schnettler, R.; Kobe, S.; Novak, S. Enhanced Osteogenesis on Titanium Implants by UVB Photofunctionalization of Hydrothermally Grown TiO_2 Coatings. *J. Biomater. Appl.* **2014**, under revision.
(22) Gallardo-Moreno, A. M.; Pacha-Olivenza, M. A.; Fernández-Calderón, M.-C.; Pérez-Giraldo, C.; Bruque, J. M.; González-Martín, M.-L. Bactericidal Behaviour of Ti6Al4V Surfaces after Exposure to UV-C Light. *Biomaterials* **2010**, *31*, 5159−5168.
(23) Shiraishi, K.; Koseki, H.; Tsurumoto, T.; Baba, K.; Naito, M.; Nakayama, K.; Shindo, H. Antibacterial Metal Implant with a TiO_2-Conferred Photocatalytic Bactericidal Effect against *Staphylococcus aureus*. *Surf. Interface Anal.* **2009**, *41*, 17−22.
(24) Suketa, N.; Sawase, T.; Kitaura, H.; Naito, M.; Baba, K.; Nakayama, K.; Wennerberg, A.; Atsuta, M. An Antibacterial Surface on Dental Implants, Based on the Photocatalytic Bactericidal Effect. *Clin. Implant Dent. Relat. Res.* **2005**, *7*, 105−111.
(25) Lorenzetti, M.; Biglino, D.; Novak, S.; Kobe, S. Photoinduced Properties of Nanocrystalline TiO_2-Anatase Coating on Ti-Based Bone Implants. *Mater. Sci. Eng., C* **2014**, *37*, 390−398.
(26) Fujishima, A.; Rao, T. N.; Tryk, D. A. Titanium Dioxide Photocatalysis. *J. Photochem. Photobiol., C* **2000**, *1*, 1−21.
(27) Katsikogianni, M.; Missirlis, Y. F. Concise Review of Mechanisms of Bacterial Adhesion to Biomaterials and of Techniques Used in Estimating Bacteria−Material Interactions. *Eur. Cells Mater.* **2004**, *8*, 37−57.
(28) Bruinsma, G. M.; van der Mei, H. C.; Busscher, H. J. Bacterial Adhesion to Surface Hydrophilic and Hydrophobic Contact Lenses. *Biomaterials* **2001**, *22*, 3217−3224.
(29) Gallardo-Moreno, A. M.; Pacha-Olivenza, M. A.; Saldaña, L.; Pérez-Giraldo, C.; Bruque, J. M.; Vilaboa, N.; González-Martín, M. L. In Vitro Biocompatibility and Bacterial Adhesion of Physico-Chemically Modified Ti6Al4V Surface by Means of UV Irradiation. *Acta Biomater.* **2009**, *5*, 181−192.
(30) Dong, X.; Tao, J.; Li, Y.; Zhu, H. Oriented Single Crystalline TiO_2 Nano-Pillar Arrays Directly Grown on Titanium Substrate in Tetramethylammonium Hydroxide Solution. *Appl. Surf. Sci.* **2010**, *256*, 2532−2538.
(31) Drnovšek, N.; Rade, K.; Milačič, R.; Štrancar, J.; Novak, S. The Properties of Bioactive TiO_2 Coatings on Ti-Based Implants. *Surf. Coat. Technol.* **2012**, *209*, 177−183.
(32) Li, B.; Logan, B. E. Bacterial Adhesion to Glass and Metal−Oxide Surfaces. *Colloids Surf., B* **2004**, *36*, 81−90.
(33) Boks, N. P.; Norde, W.; van der Mei, H. C.; Busscher, H. J. Forces Involved in Bacterial Adhesion to Hydrophilic and Hydrophobic Surfaces. *Microbiology* **2008**, *154*, 3122−3133.
(34) Poortinga, A. T.; Bos, R.; Norde, W.; Busscher, H. J. Electric Double Layer Interactions in Bacterial Adhesion to Surfaces. *Surf. Sci. Rep.* **2002**, *47*, 1−32.
(35) van Oss, C. J. *Interfacial Forces in Aqueous Media*. Marcel Dekker: New York, 1994.

DOI: 10.1021/am507148n
ACS Appl. Mater. Interfaces 2015, 7, 1644−1651